Electronic structure and the thermoelectric power of

$Na_{0.6}CoO_2$ and $Ca_3Co_4O_9$ layered cobalt oxides

Takio Kitao[1], Tsunehiro Takeuchi[1,2], Takeshi Kondo[1,2], Hiroshi Ikuta[1]
Masashi Mikami[3], Masahiro Shikano[4] and Ryoji Funahashi[4]

[1]Department of Crystalline Materials Science, Nagoya University, Nagoya 464-8603, JAPAN
[2]EcoTopia Science Institute, Nagoya University, Nagoya 464-8603, JAPAN
[3]National Institute of Advanced Industrial and Technology Chubu, Nagoya 463-8560, JAPAN
[4]National Institute of Advanced Industrial and Technology Kansai, Ikeda 563-8577, JAPAN
Fax: 81-052-789-4463, e-mail: kitao@mizu.xtal.nagoya-u.ac.jp

Angle resolved photoemission spectroscopy (ARPES) with synchrotron radiation as an incident photon source was performed on the two different layered cobalt oxides, $Na_{0.6}CoO_2$ and $Ca_3Co_4O_9$. The energy–momentum dispersion was clearly observed in the ARPES spectra, strongly indicating the presence of extended and coherent Bloch states, and consequently the Boltzmann-type electrical conduction. The electronic structure near the Fermi level (E_F) in the $Ca_3Co_4O_9$ was assigned not to be those from the Ca_2CoO_3 rock-salt layers but consisting of the a_{1g} and e'_g bands from the CoO_2 layers in the same manner as in the $Na_{0.6}CoO_2$. The topology of the measured bands was essentially the same with the calculated one for the $Na_{0.6}CoO_2$, but the energy width of the bands was greatly reduced to less than 60% of the calculated ones in both compounds due most likely to the strong electron-correlation. Making full use of the measured electronic structure, we succeeded in accounting for mechanism of the coexistence of a metallic electrical conduction with a large thermoelectric power in the $Na_{0.6}CoO_2$.

Key words: ARPES, electronic structure, thermoelectric power, $Ca_3Co_4O_9$, Na_xCoO_2

Introduction

Layered cobalt oxides with CoO_2 triangular-lattice consisting of edge-shared CoO_6 octahedrons have attracted a great deal of interests because of their possession of a large thermoelectric power with a metallic electrical conduction [1-8]. Some of these cobalt oxides also possess a low thermal conductivity due most likely to the misfit structure between the CoO_2 layers and the interstitial layers [2,6]. Since the large thermoelectric power S and the large electrical conductivity σ together with the low thermal conductivity κ are of necessities for practical thermoelectric materials, these layered cobalt oxides have been regarded as promising candidates for the practical thermoelectric materials.

In order to understand the mechanism leading to the large S with the metallic electrical conduction, we have investigated valence band structure of the layered cobalt oxides in our previous work using the Co $2p$-$3d$ resonant photoemission spectroscopy and high-resolution ultraviolet photoemission spectroscopy measurements. As a result of these experiments, we concluded that the electronic structure near the Fermi level (E_F) is characterized by narrow bands of less than 2 eV in energy width with their edge near E_F, and that this unique electronic structure is responsible for the coexistence of the large thermoelectric power and the metallic electrical conduction in these layered cobalt oxides [9,10].

In this study, we performed angle resolved photoemission spectroscopy (ARPES) on the layered cobalt oxides, $Na_{0.6}CoO_2$ and $Ca_3Co_4O_9$, in order to further confirm the role of the electronic structure in enhancing the thermoelectric power of these two layered cobalt oxides. Energy-momentum (E - k) dispersion near E_F was investigated in detail and the electronic density of states $N(E)$ was calculated from the measured E-k dispersion. By calculating $S(T)$ from the determined E-k dispersion in the context of the Boltzmann transport equation, we discuss the mechanism for the large $S(T)$ in terms of the precisely determined electronic structure.

Experimental Procedure

High-quality single crystals of $Na_{0.6}CoO_2$ and $Ca_3Co_4O_9$ were grown by the flux method. Details of the sample preparation were reported elsewhere [6,8]. Angle resolved photoemission spectroscopy (ARPES) measurements with an incident energy of hv = 22 eV were carried out at the port 011 Undulator-4mNIM in the Synchrotron Radiation Center, Wisconsin. We used Gammadata-Scienta SES2002 hemispherical analyzer for the ARPES measurements with an energy resolution of about 20 meV, which was estimated as the energy width of the intensity reduction from 90 to 10 % at the Fermi level of the reference gold. The angular resolution employed in this study was 0.45°. Although the best angular resolution of the SES2002 is better than 0.1°, we intentionally lowered the resolution to increase the signal intensity. The employed angular resolution of 0.45° is small enough as it corresponds to 0.6% of the primitive reciprocal lattice vector $|G|$ = $4\pi/\sqrt(3a)$ of the two-dimensionally extended CoO_2 triangular lattice, where a represents the distance between the nearest cobalt atoms in the CoO_2 planes. The orientation of the single crystal was determined using x-ray Laue pictures, and the crystals were precisely mounted on the ARPES sample holder within an accuracy of ±0.5°. A clean surface was prepared by cleaving the samples under an ultrahigh vacuum atmosphere with a base pressure better than 1×10^{-10} torr. ARPES spectra were measured at 40K along two high-symmetry lines; Γ-M and Γ-K. The atomic arrangements in a CoO_2 triangular lattice and the
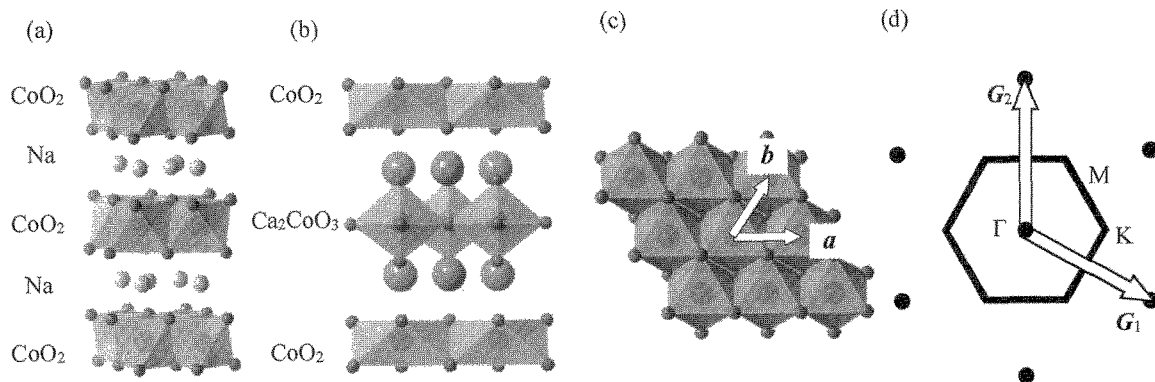
(a)   (b)   (c)   (d)

Fig.1. Schematic illustration of the layered structure in (a) Na_xCoO_2 and (b) $Ca_3Co_4O_9$. Two dimensionally extended CoO_2 layer and its corresponding first Brillouin zone are shown in (c) and (d), respectively.

corresponding hexagonal Brillouin zone are schematically drawn in Figs.1 (a) ~ (d).

Results

Since electron transport properties are dominated by the bands that cross E_F, it must be of great importance to investigate the electronic structure in the vicinity of E_F in detail. In this study, therefore, we concentrate on revealing the electronic structure only in the energy range of a few eV about E_F.

The second energy-derivative of the ARPES intensity at the Γ-K direction is shown in Fig.2 in the energy range from 0.2 to -1.4 eV. Dispersion of the eigen value with varying momentum was clearly observed in both compounds. This experimental fact indicates that the single crystals we employed in the present

measurement have excellent quality over the whole radiation-area of the incident photon-beam (~φ100 μm), and that the wave function of the electrons in the valence band are well explained with the extended Bloch waves rather than by the localized atomic orbitals. The Boltzmann-type electrical conduction mechanism is also suggested for these layered cobalt oxides.

First principle band calculations predicted that the bands in the vicinity of E_F of the $Ca_3Co_4O_9$ consist of atomic orbitals in the Ca_2CoO_3 rock-salt layers [11], while those of the Na_xCoO_2 are characterized by the components from the CoO_2 layers [12]. Fairly different band-dispersions were expected near E_F for these two cobalt oxides, however the observed bands of these two compounds resemble each other in their periodicity and topology. The bands with strong intensity in both
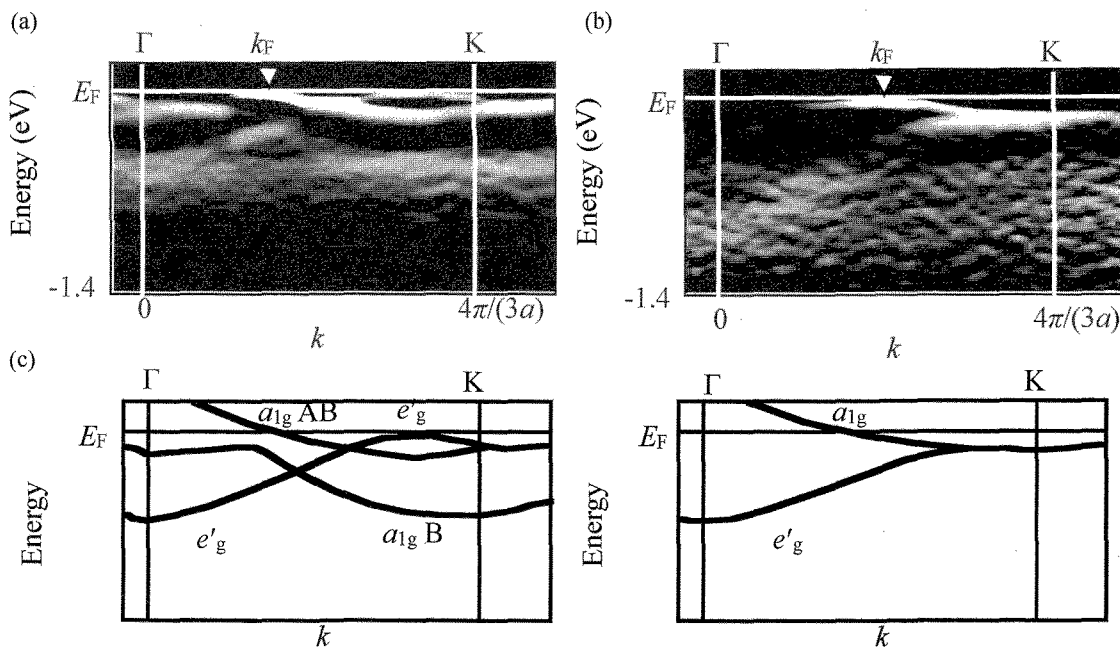

Fig.2. Second energy derivative of the ARPES intensity ($d^2I(k,E)/dE^2$) along the Γ-K direction in the energy range of 0.2~-1.4eV for (a) $Na_{0.6}CoO_2$ and (b) $Ca_3Co_4O_9$. The bands with strong intensity in both compounds have essentially the same E-k dispersion, assigned as a_{1g} and e'_g bands, which were schematically drown in (c). "B" and "AB" indicate bonding and anti-bonding bands, respectively, caused by the hybridization between two CoO_2 layers in the unit cell .
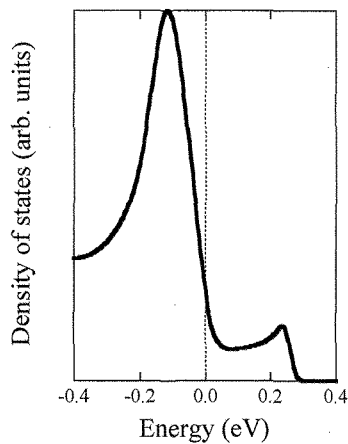
Fig.3. Electronic density of states of $Na_{0.6}CoO_2$ calculated from the experimentally determined *E-k* dispersion. Band edge is located about 0.3 eV above E_F, and a van Hove singularity is observable at about -0.15 eV.

compounds were found to possess essentially the same topology of the calculated a_{1g} and e'_g bands consisting of Co $3d$ and O $2p$ components in the CoO_2 layers reported for $Na_{0.5}CoO_2$ [12]. Therefore we safely assigned those bands as a_{1g} and e'_g bands from the CoO_2 layers. This assignment is fully consistent with our previously reported arguments on the basis of the angle integrated photoemission spectroscopy measurements [9]. It is of great importance to stress here that the conduction electrons of the $Ca_3Co_4O_9$ do not wander in the Ca_2CoO_3 rock-salt layers but only in the CoO_2 layers similarly to the conduction electrons in the Na_xCoO_2.

Notably, the e'_g band does not cross the Fermi level even though it comes up to 20 meV below E_F at $k\sim0.8k_K$ where presence of a small hole pocket was predicted by the band calculation. On the other hand, the a_{1g} band certainly produces large hole-like Fermi surface centered at the Γ point. We strongly argue on the basis of these experimental facts that the electrical conduction in these cobalt oxides is dominantly caused by the a_{1g} band of the CoO_2 planes especially at low temperatures.

We also realized that the energy width of the measured bands is less than 60% of the calculated ones. Since the reduction in the band-width known as the "mass-renormalization effect" is caused by the strong electron-correlation, electron-correlation in these layered cobalt oxides are naturally considered to be very strong. The width of the bands in the $Na_{0.6}CoO_2$ is slightly smaller than that of the $Ca_3Co_4O_9$, indicating a slightly stronger electron-correlation in the $Na_{0.6}CoO_2$.

Discussions

In this section, the reason for the simultaneous achievement of the large thermoelectric power and the metallic electrical conduction in the layered cobalt oxides is discussed in terms of the electronic structure near E_F using the ARPES data measured for the $Na_{0.6}CoO_2$.

Energy-momentum (*E-k*) dispersion of the $Na_{0.6}CoO_2$ was determined by taking the peak momentum k_{peak} in the momentum distribution curves $I_E(k)$ which were obtained by cutting the ARPES
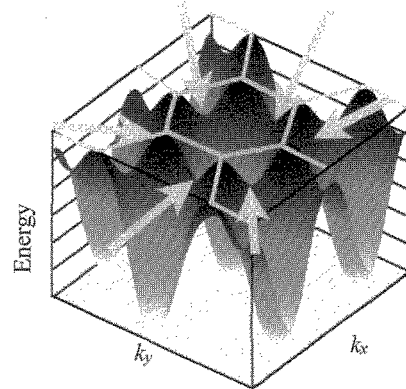

Fig.4. Topology of the e'_g band determined by tight-binding function fitting for the $Na_{0.6}CoO_2$. Saddle points indicated by the arrows were observable in the hexagonal 1st Brillouin zone.

intensity $I(E,k)$ at a given energy E. The k_{peak} providing the peak momentum in each $I_E(k)$ was precisely determined by a Lorentzian-function fitting [10]. By using the data sets of *E-* k_{peak} dispersion thus determined, we performed tight-binding function fitting for the two-dimensional triangular lattice with ignoring the complicated bi-layer-splitting that is caused by the hybridization between two CoO_2 layeres in the unit cell.

The fitting functions we employed in this work are

$$E = E_0 + 2t\left\{\cos\left(2k_x / \sqrt{3}\right) + 2\cos\left(k_x / \sqrt{3}\right)\cos\left(k_y\right)\right\}$$
$$+ 2t'\left\{\cos\left(4k_x / \sqrt{3}\right) + 2\cos\left(2k_x / \sqrt{3}\right)\cos\left(2k_y\right)\right\}$$
$$+ 2t''\left\{\cos\left(2k_y\right) + 2\cos\left(\sqrt{3}k_x\right)\cos\left(k_y\right)\right\}. \quad (1)$$

Here t, t' and t'' represent the transfer integral between atomic/molecular orbitals connected with a, $2a$, and $a+b$, respectively. The vectors a and b denote the primitive vectors in the two-dimensional triangular lattice.

Electronic density of states near the Fermi level N (E) was calculated from the *E-k* dispersion obtained by the tight-binding fitting. The resulting $N(E)$ are shown in Fig. 3. We previously argued on the basis of the angle integrated photoemission measurements that (a) the presence of the band edge just above E_F and (b) the steeply increasing $N(E)$ with decreasing energy just below E_F are responsible for the large thermoelectric power of the layered cobalt oxides.[9] These two features are obviously reproduced in the calculated $N(E)$ shown in Fig.4. It is realized as a consequence of the tight-binding fitting that the feature (b) is caused by the less dispersive e'_g band that possesses a van Hove singularity (vHs) at 0.15~0.25 eV below E_F. This vHs is brought about by the saddle point at the middle point between K and M as shown in Fig.4.

Thermoelectric power is calculated by using the following formula

$$S(T) = \frac{1}{eT}\frac{\int_{-\infty}^{\infty}\sigma(E)(E-\mu)\frac{\partial f(E)}{\partial E}dE}{\int_{-\infty}^{\infty}\sigma(E)\frac{\partial f(E)}{\partial E}dE}. \quad (2)$$

Here $\sigma(E)$ and $f(E)$ represent the contribution of electrons at the energy E to the electrical conductivity (spectral conductivity) and the Fermi-Dirac distribution
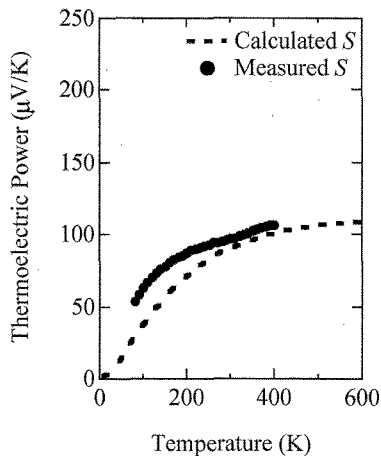
Fig.5. Measured [REF.8] and calculated $S(T)$ of
$Na_{0.6}CoO_2$. The calculated $S(T)$ plotted with dashed
line shows quantitative agreement with the
measured one.

function, respectively. If the mean free path of the conduction electrons is energy-independent in the vicinity of E_F and the electronic structure in the CoO_2 planes is isotropic, Eq. (2) can be transformed into

$$S(T) = \frac{1}{eT} \frac{\int_{-\infty}^{\infty} v(E)N(E)(E-\mu)\frac{\partial f(E)}{\partial E} dE}{\int_{-\infty}^{\infty} v(E)N(E)\frac{\partial f(E)}{\partial E} dE}, \quad (3)$$

where $v(E)$ and $N(E)$ denote the group velocity and the density of states, respectively [13]. Nearly circular shape of the Fermi surface reported for the Na_xCoO_2 by Yang et al. [14] lends a support to the assumption of the two-dimensionally isotropic electronic structure. The energy independent mean free path is also appropriate, because the shape of the momentum distribution curves, which directly reflects the mean free path, was almost energy independent at $E_F < E < \sim 40meV$ for the $Ca_3Co_4O_9$ [15]. Since both $v(E)$ and $N(E)$ had already determined by the present ARPES measurements and the subsequent tight-binding fitting, we calculated $S(T)$ using those data with Eq.(3). The resulting $S(T)$ are plotted in Fig.5 together with measured one. Obviously the calculated thermoelectric power shows fairly good consistency with the measured one not only in the magnitude but also in its temperature dependence. It is found as a consequence of the $S(T)$ calculation that the large positive thermoelectric power is caused by the large density of states at $100\sim200$ meV below E_F, i.e., by the presence of the vHs in the e'_g band.

Conclusion

Angle resolved photoemission spectroscopy with synchrotron radiation photon source was performed on two different layered cobalt oxides; $Na_{0.6}CoO_2$ and $Ca_3Co_4O_9$. The measured electronic structure near the Fermi level in the $Na_{0.6}CoO_2$ showed a fairly good consistency with the theoretically predicted one, while the $Ca_3Co_4O_9$ showed certainly different electronic structure from the theoretical calculation by possessing essentially the same topology of band structure with those of the $Na_{0.6}CoO_2$. Conduction electrons both in the $Na_{0.6}CoO_2$ and $Ca_3Co_4O_9$, therefore, are considered to

wander in the CoO_2 layers. It is also confirmed that the strong electron correlation effectively reduces the energy width of the bands in both compounds. $S(T)$ in the $Na_{0.6}CoO_2$ was calculated from the bands determined by the measured ARPES data within the framework of the Bolzmann transport theory. The calculated $S(T)$ quantitatively reproduced the measured one. The present analysis revealed that the large thermoelectric power is caused by the large density of states at the vHs in the e'_g band, while the metallic conduction is brought about by the a_{1g} band.

References

[1] I. Terasaki, Y. Sasago and K. Uchinokura, *Phys. Rev. B* **56** (1997) pp. R12685-12687.

[2] R. Funahashi, I. Matsubara, H. Ikuta, T. Takeuchi, U. Mizutani and S. Sodeoka, *Jpn. J. Appl. Phys.* **39** (2000) pp. L1127-L1129.

[3] A. Maignan, S. Hébert, M. Hervieu, C. Michel, D. Pelloquin, and D. Khomskii, *J. Phys. Condens. Matter* **15** (2003) pp.2711-2723.

[4] A.C. Masset, C. Michel, A. Maignan, M. Hervieu, O. Toulemonde, F. Studer, B. Raveau and J. Hejtmanek, *Phys. Rev. B* **62** (2000) pp. 166-175.

[5] K. Fujita, T. Mochida and K. Nakamura, *Jpn. J. Appl. Phys.* **40** (2001) pp.4644-4647.

[6] M. Shikano and R. Funahashi, *Appl. Phys. Lett.* **82** (2003) pp.1851-1853.

[7] S. Hébert, S. Lambert, D. Pelloquin and A. Maignan, *Phys. Rev. B* **64** (2001) pp.172101 1-4.

[8] M. Mikami, M Yoshimura, Y. Mori, T. Sasaki, R. Funahashi and M. Shikano, *Jpn. J. Appl. Phys.* **42** (2003) pp.7383-7386.

[9] T. Takeuchi, T. Kondo, T. Takami, H. Takahashi, H. Ikuta, U. Mizutani, R. Funahashi, M. Shikano, M. Mikami, S. Tsuda, T. Yokoya, S. Shin and T. Muro, *Phys. Rev. B* **69** (2004) pp.125410 1-9.

[10] T. Takeuchi, T. Kondo, T. Kitao, K. Soda, M. Shikano, R. Funahashi, M. Mikami and U. Mizutani, *J. Electron Spectrosc. Relat. Phenom.* **137-140** (2004) pp. 595-599.

[11] R. Asahi, J. Sugiyama and T. Tani, *Phys. Rev. B* **66** (2002) pp.155103 1-7.

[12] D. J. Singh, *Phys. Rev. B* **61** (2000) pp.13397-13402.

[13] T. Kondo, T. Takeuchi, U. Mizutani, T. Yokoya, S. Tsuda and S. Shin, *Phys. Rev. B* 72, pp. 024533 1-9.

[14] H.-B. Yang, Z.-H. Pan, A. K. P. Sekharan, T. Sato, S. Souma, T. Takahashi, R. Jin, B. C. Sales, D. Mandrus, A. V. Fedorov, Z. Wang and H. Ding, *Phys. Rev. Lett.* **95** (2005) pp.146401 1-4.

[15] T. Takeuchi, T. Kondo, T. Kitao, K. Soda, M. Shikano, R. Funahashi, M. Mikami and U. Mizutani, *J. Electron Spectrosc. Relat. Phenom.* **144-147** (2005) pp. 849-852.